

EMAGE: Towards Unified Holistic Co-Speech Gesture Generation via Expressive Masked Audio Gesture Modeling

Haiyang Liu^{1*} Zihao Zhu^{2*} Giorgio Becherini³ Yichen Peng⁴ Mingyang Su⁵
 You Zhou Xuefei Zhe Naoya Iwamoto Bo Zheng Michael J. Black³

¹The University of Tokyo ²Keio University
³Max Planck Institute for Intelligent Systems ⁴JAIST ⁵Tsinghua University

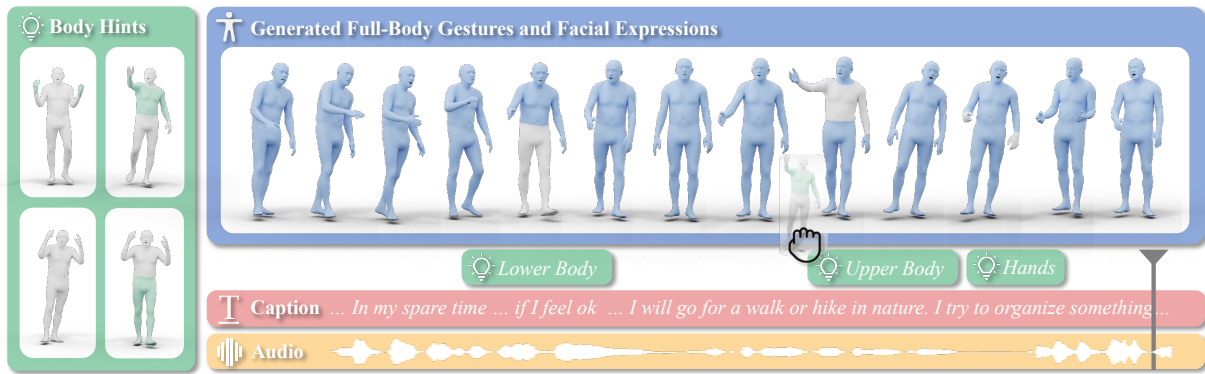


Figure 1. **EMAGE**. We present a Masked Audio-Conditioned Gesture Modeling framework, along with a new holistic gesture dataset, BEAT2 (BEAT-SMPLX-FLAME), for jointly generating **facial expressions**, **local body dynamics**, **hand movements** and **global translations**, conditioned on audio and a partially or completely masked **gestures**. The gray denotes visible gestures, and blue represents our outputs.

Abstract

We propose *EMAGE*, a framework to generate full-body human gestures from audio and masked gestures, encompassing facial, local body, hands, and global movements. To achieve this, we first introduce BEAT2 (BEAT-SMPLX-FLAME), a new mesh-level holistic co-speech dataset. BEAT2 combines a MoShed SMPL-X body with FLAME head parameters and further refines the modeling of head, neck, and finger movements, offering a community-standardized, high-quality 3D motion captured dataset. EMAGE leverages masked body gesture priors during training to boost inference performance. It involves a Masked Audio Gesture Transformer, facilitating joint training on audio-to-gesture generation and masked gesture reconstruction to effectively encode audio and body gesture hints. Encoded body hints from masked gestures are then separately employed to generate facial and body movements. Moreover, EMAGE adaptively merges speech features from the audio’s rhythm and content and utilizes four compositional VQ-VAEs to enhance the results’ fidelity and diversity. Experiments demonstrate that EMAGE generates

holistic gestures with state-of-the-art performance and is flexible in accepting predefined spatial-temporal gesture inputs, generating complete, audio-synchronized results. Our code and dataset are available.¹

1. Introduction

The path towards full-body co-speech gesture generation presents many remaining challenges. Despite the development of various baselines, e.g., audio conditioned models for face [15, 20, 61], body [13, 25, 67], and hand movements [33, 39, 41], along with a few attempts at merged models [28, 65], the limited availability of comprehensive data and models poses an ongoing obstacle. To make progress in this direction, we present a new framework that can incorporate partial spatial-temporal predefined gestures and autonomously complete the remaining frames in synchronization with the audio. This provides a new tool for creating realistic animations of digital humans

*Equal Contribution.

¹<https://pantomatrix.github.io/EMAGE/>

[57, 63, 64, 71].

To achieve this, we first require a comprehensive gesture dataset. While several datasets are available for audio-to-body [67], audio-to-body&face [28], body-to-hands [39, 41], and common actions [16, 46], integrating them poses challenges due to varying data formats and evaluation metrics across different sub-areas. This motivates us to establish a unified, community-standard benchmark for training and evaluating holistic gestures. We build upon the BEAT dataset [39], which provides the most comprehensive mocap co-speech gesture dataset with diverse modalities. Despite its size and richness, the data in BEAT is not presented in a standardized format. The dataset comprises iPhone ARKit blendshape weights and Vicon skeletons, posing challenges when using the data for training; *e.g.*, the lack of a mesh representation prevents the use of a vertex loss [19, 52]. Additionally, conducting direct human perceptual evaluations on these diverse modalities is inherently complex. On the other hand, SMPL-X [50] and FLAME [35] are common mesh standards for the academic community for other human dynamics-related tasks, *e.g.*, action [52] and talking head generation [14]. Driven by the motivation to facilitate the sharing of knowledge across different tasks, we present BEAT-SMPLX-FLAME (BEAT2), which consists of two main components: **i)** Refined SMPL-X body shape and pose parameters from MoSh++ [44, 46] with hard-coded physical priors. **ii)** Optimized high-quality FLAME head parameters. By integrating SMPL-X’s body and FLAME’s head, BEAT2 facilitates a comprehensive training and evaluation benchmark across multiple sub-areas of co-speech human animation generation.

With the holistic data from BEAT2, we aim to enhance the coherence of individual body parts while ensuring accurate cross-modal alignment between audio and motion; see Figure 1. This leads to the design of Expressive Masked Audio-conditioned GESture modeling, denoted as EMAGE, a spatial and temporal transformer-based framework. EMAGE first aggregates spatial features from masked body joints. Then, it reconstructs the latent space of pretrained gestures with a switchable gesture temporal self-attention and audio-gesture cross-attention. The selection of different forward paths enables modeling the gesture-to-gesture and audio-to-gesture prior separately and effectively. Once the reconstructed latent features are obtained, EMAGE decodes local face and body gestures from four compositional pretrained Vector Quantized-Variational AutoEncoders (VQ-VAEs) and decodes global translations from a pretrained Global Motion Predictor. The compositional VQ-VAEs are key to preserving audio-related motions during the reconstruction. Through these designs, EMAGE achieves state-of-the-art performance in generating body and face gestures. It takes as input audio and partially initialized gestures, and recovers audio-

synchronized, coherent gestures. Additionally, we show how EMAGE can flexibly incorporate additional, non-holistic, datasets to improve results.

Overall, our contributions are as follows: (1) We release BEAT2, a representation-unified, mesh-level dataset that leverages MoShed SMPL-X body and FLAME head parameters. (2) We propose EMAGE, a simple yet effective holistic gesture generation framework that generates coherent gestures with partial gesture and audio priors. (3) EMAGE achieves state-of-the-art performance in generating both body and face gestures with only four frames of seed gestures. (4) EMAGE showcases the use of additional non-holistic gesture datasets for training, *e.g.*, Trinity and AMASS, to further improve the fidelity and diversity of the results, effectively leveraging data from different datasets.

2. Related Work

Co-Speech Animation Datasets are categorized into two types; see Table 1: pseudo-labeled (PGT) and motion-captured (mocap). For PGT, the Speech2Gesture Dataset [25] utilizes OpenPose [11] to extract 2D poses from News and Teaching videos. Subsequent works extend the dataset to 3D pose [28] and SMPL-X [65]. The TED Dataset [66], which extracts 2D pose from TED videos, has been extended to include 3D pose [67], fingers [40], and SMPL-X [45]. Similarly, 2D, 3D landmarks, and meshes are estimated from multi-view recorded videos [60] as PGT for talking-head generation. Although pseudo-labeled approaches could theoretically extract infinite data, their accuracy is limited. For instance, the average error (in mm) for the SOTA monocular 3D pose estimation algorithm [23] on the Human3.6M dataset [30] is 33.4, while for Vicon mocap it is 0.142 [47]. For mocap datasets, Trinity [3] features one male actor with 4h of data, and TalkingWithHands [32] collects conversation scenarios for two speakers. ZEEG [24] considers one speaker with 12 styles. For the face, 3D scanning is accurate but limited in quantity due to cost, *e.g.*, less than 3h for BIWI [21], VOCA [14], and MeshTalk [56]. This leads to a balance between performance and quantity in the ARKit dataset [51]. The aforementioned datasets address the body and face separately. On the other hand, BEAT [39] includes both 3D pose body and ARKit [8] facial blendshape weights for the first time. However, BEAT lacks mesh data.

Co-Speech Animation Models are categorized based on their outputs; see Table 2. In addition to the baselines and datasets [14, 25, 32, 48, 56, 67], several frameworks for body gestures [2, 33, 53, 54] have improved the performance of the baselines. They are trained and evaluated by selecting specific upper body joints [4, 5, 38–40, 49, 70], or all body joints [62, 72]. Recent improvements in facial gestures drive the vertices with transformers and discrete face priors [19, 61]. However, these methods only address ei-

	Trinity Mocap 2017 [22]	S2G S2G-2D 2019 [25]	Seq2Seq TED-2D 2019 [66]	TWH Mocap 2019 [32]	Trimodal TED-3D 2020 [67]	VOCA Scan 2020 [14]	MeshTalk Scan 2021 [56]	Hahibie <i>et al.</i> S2G-3D 2021 [28]	HA2G TED-3D+ 2022 [40]	BEAT Mocap 2022 [39]	ZEEG Mocap 2022 [24]	Yoon. <i>et al.</i> TED-SMPL 2023 [45]	Talkshow S2G-SMPL 2023 [65]	BEAT2 Ours 2024
Head	-	2D	-	-	-	3D Scan	3D Scan	3D	-	ARKit	-	-	PGT-Mesh	MC-Mesh
Upper Body	3D	2D	2D	3D	3D	-	-	3D	3D	3D	3D	PGT-Mesh	PGT-Mesh	MC-Mesh
Hands	3D	2D	-	3D	-	-	-	3D	3D	3D	3D	PGT-Mesh	PGT-Mesh	MC-Mesh
Lower Body	3D	-	-	3D	-	-	-	-	-	3D	3D	-	-	MC-Mesh
Global Motion	3D	-	-	3D	-	-	-	-	-	3D	3D	-	-	MC-Mesh
Duration (hours)	4	60	97	20	97	0.5	2	38	33	76	4	30	27	60

Table 1. **Comparison of Co-Speech Gesture Datasets.** We summarize gesture and face datasets in talking scenarios. ‘PGT’ and ‘MC’ denote Pseudo Ground Truth and Motion Capture, respectively. The BEAT2 (Ours) dataset is the largest dataset for motion-captured data, providing holistic, academic community standard mesh-level information.

	S2G 2019 [25]	TriModal 2020 [67]	B2H 2020[48]	TWH 2021[32]	Hahibie <i>et al.</i> 2021[28]	DisCo 2022[38]	HA2G 2022[40]	Face Former 2022[19]	Rhythmic 2022[5]	BEAT CaMN 2022[39]	Diff Gesture 2023[72]	Code Talker 2023[61]	Talk Show 2023[65]	DiffStyle Gesture 2023[62]	Body Former 2023[49]	Lively Speaker 2023[70]	EMAEG (Ours) 2024
Input Gestures	-	-	Body	Body	-	-	-	-	-	-	-	-	-	-	-	-	Masked
Head	-	-	-	-	M	-	-	S	-	-	-	S	-	-	-	-	C
Upper	S	S	-	-	M	S	C	-	S	C	S	-	C	S	S	S	C
Hands	-	-	S	S	M	S	C	-	-	C	S	-	C	S	-	S	C
Lower + Global	-	-	-	-	-	-	-	-	-	-	-	-	-	S	-	-	C

Table 2. **Comparison of Co-Speech Gesture Models.** We compare with previous methods for generating face or body motion trained on co-speech datasets. The first row lists their inputs, and the subsequent rows list their outputs, respectively. Different decoder designs are denoted by the initials ‘S’ for Single, ‘M’ for Multiple, and ‘C’ for Cascaded. To the best of our knowledge, EMAGE (Ours) is the first to accept audio and partially or completely masked gestures, generating full-body audio-synchronized results.

ther the face or body. Applying these methods to the full body will yield sub-optimal results as audio is differently correlated with face and body dynamics. Most similar to our work, Hahibie *et al.* [28] employ a single audio encoder and multiple decoders for generating face and body gestures. TalkSHOW [65] demonstrates the advantage of separating the audio encoders and decoding the body and hands using quantized codes in an auto-regressive manner. However, it lacks lower body and global motion, and there is no shared information for body and facial gesture generation. Moreover, it cannot accept partially masked body hints due to the design of a fully auto-regressive model.

Masked Representation Learning was first demonstrated to be effective in Natural Language Processing, with BERT-based models [17, 31, 42] boosting the performance of learned word embeddings in downstream tasks through a combination of masked language modeling and transformer architecture. Subsequently, Masked AutoEncoders [29] expanded masked image modeling to computer vision by removing and inpainting image patches. This concept of masked representation learning has since been employed in other modalities, *e.g.*, video [12, 18, 43], audio [26, 36, 37], and point clouds [55, 68, 69]. Most related to our work, MotionBERT [73] proposes a spatial-temporal transformer to learn a robust motion representation for classification-based tasks by masking 2D pose. In contrast to their method, we target robust motion features for conditional motion generation tasks, requiring a balance in training between multiple modalities, *e.g.*, audio and gesture.

3. BEAT2

This section introduces how we obtain unified mesh-level data, *i.e.*, SMPL-X [50] and FLAME [35] parameters, from

the original BEAT dataset [39]. BEAT utilizes a Vicon motion capture system [47] and releases 78-joint skeleton-level Biovision Hierarchy (BVH) [10] motion files. Their facial capture system uses ARKit [8] with a depth camera on the iPhone 12 Pro, extracting \mathbb{R}^{51} blendshape weights. These blendshapes are designed based on the Facial Action Coding System (FACS), which is widely adopted. However, both the motion and facial data lack mesh-level details (see Figure 2), *e.g.*, shapes and vertices.

3.1. Body Parameters Initialization via MoSh++

We initialize the SMPL-X body shape and pose parameters from BEAT mocap marker data using MoSh++ [46]. Given the captured markers positions $\mathbf{m} \in \mathbb{R}^{T \times K \times 3}$, predefined markers position offsets $\mathbf{d} \in \mathbb{R}^{K \times 3}$, and user-defined vertices-to-markers function \mathcal{H} , we aim to obtain body shape $\beta \in \mathbb{R}^{300}$, poses $\theta \in \mathbb{R}^{T \times 55 \times 3}$, and translation parameters $\gamma \in \mathbb{R}^{T \times 3}$. The optimization uses a differentiable surface vertex mapping function $\mathcal{S}(\beta, \theta, \gamma)$ and vertex normal function $\mathcal{N}(\beta, \theta_0, \gamma_0)$. For each frame, the latent marker $\tilde{\mathbf{m}} \in \mathbb{R}^{T \times K \times 3}$ is calculated as

$$\tilde{\mathbf{m}}_i \equiv \mathcal{S}_{\mathcal{H}}(\beta, \theta_i, \gamma_i) + \mathbf{d} \mathcal{N}_{\mathcal{H}}(\beta, \theta_i, \gamma_i). \quad (1)$$

We first select 12 frames to optimize and fix \mathbf{d} and β , then optimize θ_i, γ_i for $i \in (1 : T)$ by minimizing the loss terms based on $\|\tilde{\mathbf{m}}_i - \mathbf{m}_i\|^2$, including Data Term, Surface Distance Energy, Marker Initialization Regularization, Pose and Shape Priors, Velocity Constancy, and Soft-Tissue Term (see supplementary materials). The overall objective function is the weighted sum of these terms to balance accuracy and plausibility.

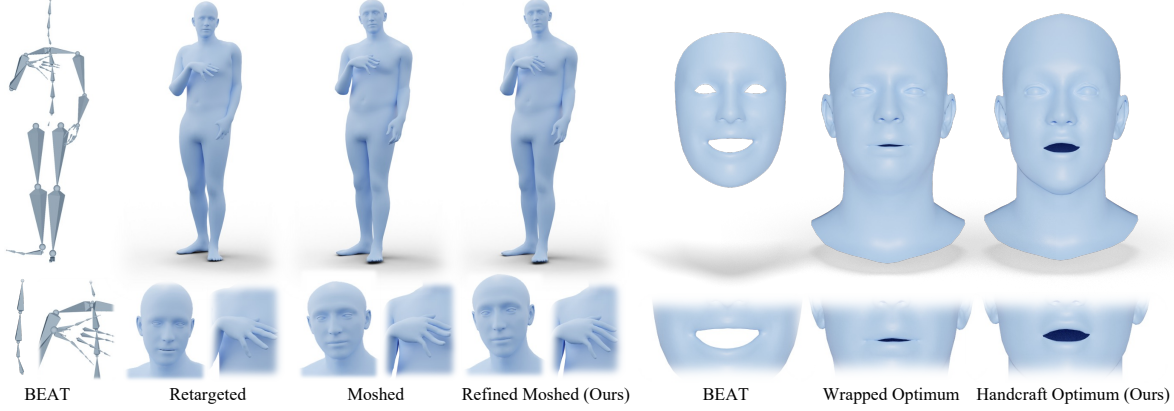


Figure 2. **Comparison of Data between BEAT2 and Others.** BEAT-SMPLX-FLAME presents a new mesh-level, motion-captured, holistic co-speech gesture dataset with 60h of data. *Left:* We compare our refined SMPL-X body parameters (denoted as Refined MoSh) with the original BEAT skeleton [39], Retargeted from AutoRegPro, and initial results of Mosh++ [50]. The refined results show correct neck flexion, appropriate head and neck shape ratios, and detailed finger representations. *Right:* Visualization of blendshape weights from the original BEAT dataset [39] with ARKit’s template, Wrapped-based, and handcrafted optimization. Our final handcrafted FLAME blendshape-based optimization demonstrates both accurate lip movement details and natural mouth shapes.

3.2. Body Parameters Refinement

MoSh++ produces unnatural head shapes due to the fact that head markers were worn on a helmet and it sometimes produces unnatural finger poses. Consequently, we refine body shape and pose parameters with three simple yet effective hard-coded physical rules. **i)** The neck and head length should approximate $1/7$ of the total length of the body. **ii)** Fingers, except for the thumb, should not bend backward. **iii)** We employ the Kolmogorov-Smirnov test, which reveals the data is similar to a normal distribution. Subsequently, we apply a Gaussian truncation approach, where all data points falling outside the 3σ range are adjusted to align with the 3σ threshold and blended with the adjacent 10 frames. We compare our refined body parameters (denoted as MoSh Refined) with Original BEAT, Retargeted SMPL-X, and MoSh SMPL-X in Figure 2.

3.3. Blendshape Weights to FLAME Parameters

Given the ARKit blendshape weights $\mathbf{b}_{\text{ARKit}} \in \mathbb{R}^{T \times 51}$, we aim to derive a transformation matrix $\mathbf{W} \in \mathbb{R}^{51 \times 103}$ that maps these into FLAME parameters $\mathbf{b}_{\text{FLAME}} \in \mathbb{R}^{T \times (100+3)}$, where 100 represents the number of dimensions for expression parameters and 3 for jaw movement. Due to discrepancies between the iPhone’s and FLAME’s template mesh topology, simply optimizing FLAME parameters by minimizing the geometric error between the ARKit template vertices and the wrapped FLAME vertices does not yield satisfactory results. Instead, we release a set of handcrafted blendshape templates $\mathbf{v}_{\text{template}} \in \mathbb{R}^{52}$ on FLAME following ARKit’s FACS configuration. This approach allows direct driving of the FLAME topology ver-

tices $\mathbf{v} \in \mathbb{R}^{T \times 5023 \times 3}$ from the given blendshape weights,

$$\mathbf{v} = \mathbf{v}_{\text{template}}^0 + \sum_{j=1}^{51} \mathbf{b}_{\text{ARKit},j} \cdot \mathbf{v}_{\text{template}}^j \quad (2)$$

where $\mathbf{b}_{\text{ARKit},j}$ is the weight of the j -th ARKit blendshape and $\mathbf{v}_{\text{template}}^j$ is the vertex position of the FLAME model template corresponding to the j -th blendshape. The term $\mathbf{v}_{\text{template}}^0$ represents the original template vertex position of the FLAME model. We optimize \mathbf{W} by minimizing $\|\tilde{\mathbf{v}}_j - \mathbf{v}_j\|_2$, where $\tilde{\mathbf{v}}$ is obtained from FLAME’s LBS $\mathcal{V}(\mathbf{b}_{\text{FLAME}})$. The comparisons between ARKit data, wrap-based, and our approach are shown in Figure 2.

4. EMAGE

We introduce the details of EMAGE, Expressive Masked Audio-Conditioned Gesture Modeling (see Figure 3). Given gestures $\mathbf{g} \in \mathbb{R}^{T \times (55 \times 6 + 100 + 4 + 3)}$, representing 55 joints in Rot6D, \mathbb{R}^{100} FLAME parameters, \mathbb{R}^4 foot contact labels, \mathbb{R}^3 global translations, and speech audio $\mathbf{a} \in \mathbb{R}^{T \times sk}$, where $sk = sr_{\text{audio}}/fps_{\text{gestures}}$, EMAGE jointly optimizes masked gesture reconstruction and audio-conditioned gesture generation. This optimization enhances performance during inference and enables the use of partially masked gestures to complete holistic gestures. To achieve this, we first model the quantized latent space in Sec. 4.1, following [61, 65]. We then design a separated speech audio encoder using Content Rhythm Self-Attention (CRA) as detailed in Sec. 4.2. Subsequently, we learn the body hints from masked gestures via the Masked Audio Gesture Transformer, explained in Sec. 4.3. Finally, the decoding strategy for different body segments is discussed in Sec. 4.4.

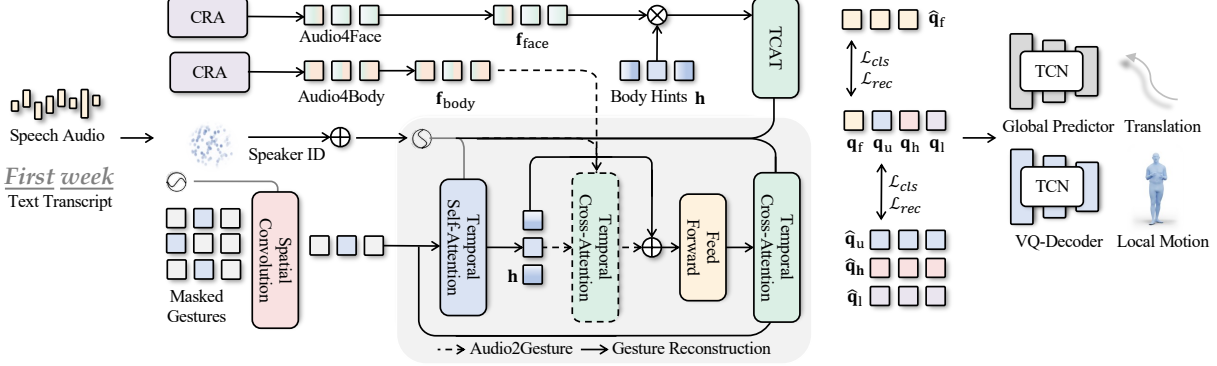


Figure 3. **EMAGE** leverages two training paths: Masked Gesture Reconstruction (MG2G) and Audio-Conditioned Gesture Generation (A2G). The MG2G path focuses on encoding robust body hints through a spatial-temporal transformer gesture encoder and cross-attention gesture decoder. In contrast, the A2G path utilizes these body hints, and separated audio encoders to decode pretrained face and body latent features. A key component in this process is a switchable cross-attention layer, crucial for merging body hints and audio features. This fusion allows the features to be effectively disentangled and utilized for gesture decoding. Once the gesture latent features are reconstructed, EMAGE employs a pretrained VQ-Decoder to decode face and local body motions. Additionally, a pretrained Global Motion Predictor is used to estimate global body translations, further enhancing the model’s capability to generate realistic and coherent gestures.

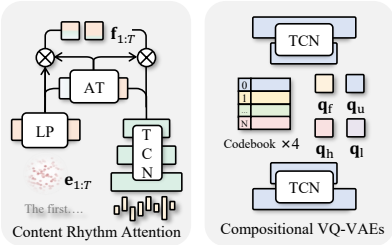


Figure 4. **Details of CRA and Pretrained VQ-VAEs.** *Left:* Content Rhythm Attention fuses speech rhythm (onset and amplitude) with content (pretrained word embeddings from text scripts) adaptively. This results in a preference for either content or rhythm in specific frames, which encourages the generation of semantical-aware gestures. *Right:* We pretrain four compositional VQ-VAEs by reconstructing face, upper body, hands and lower body separately to disentangle audio-agnostic gestures explicitly.

4.1. Compositional Discrete Face and Body Prior

We model full-body gestures in the separated quantized latent space (Figure 4) for several reasons. Similar to [65], the body and hands improves the diversity of the results. However, we additionally separate the face and lower body due to their differing correlations with audio, *i.e.*, using a single VQ-VAE to encode both the upper and lower body may lead the model to overlook gestures that occur less frequently - regardless of their relation to the audio. Specifically, a single model might focus only on recovering lower body motion, neglecting elbow movements in a speaker who is constantly walking during the conversation.

The separated quantized latent space $Q = \{q_f, q_u, q_h, q_l\}$ for the Face $g_f \in \mathbb{R}^{T \times 106}$, Upper

body $g_u \in \mathbb{R}^{T \times 78}$, Hands $g_h \in \mathbb{R}^{T \times 180}$, and Lower body $g_l \in \mathbb{R}^{T \times (54+4)}$ are from four VQ-VAEs. The VQ-VAE for each is optimized by jointly optimizing the following loss terms,

$$q_i = \arg \min_{q_i \in \mathcal{Q}} \|z_j - q_i\|^2 \quad (3)$$

$$\begin{aligned} \mathcal{L}_{\text{VQ-VAE}} = & \mathcal{L}_{\text{rec}}(\mathbf{g}, \hat{\mathbf{g}}) + \mathcal{L}_{\text{vel}}(\mathbf{g}', \hat{\mathbf{g}}') + \mathcal{L}_{\text{acc}}(\mathbf{g}'', \hat{\mathbf{g}}'') \\ & + \|\text{sg}[\mathbf{z}] - \mathbf{q}\|^2 + \|\mathbf{z} - \text{sg}[\mathbf{q}]\|^2, \end{aligned} \quad (4)$$

where \mathbf{z} is the encoded \mathbf{g} with a temporal window size $w = 1$. \mathcal{L}_{rec} , \mathcal{L}_{vel} , and \mathcal{L}_{acc} are Geodesic [58] and L1 losses, sg is a stop gradient operation, we set the weight of the commitment loss [59] (the last term) to 1 in this paper.

4.2. Content and Rhythm Self-Attention

Given the speech audio, \mathbf{s} , inspired by [4], we employ onset \mathbf{o} and amplitude \mathbf{a} as explicit audio rhythm, alongside the pretrained embeddings [9] \mathbf{e} from transcripts as content. Different from previous approaches, which typically add the rhythm and content features, we leverage self-attention to merge these features adaptively. This approach is driven by the observation that for specific frames, the gestures are more related to content (semantic-aware) or rhythm (beat-aware). The rhythm and content features are first encoded into time-aligned features $\mathbf{r}_{1:T}$ and $\mathbf{c}_{1:T}$, using a Temporal Convolutional Network (TCN) and linear mapping, respectively. For each time step $t \in \{1, \dots, T\}$, we merge the rhythm and content features by:

$$\begin{aligned} \mathbf{f}_{1:T} = & \alpha \times \mathbf{r}_{1:T} + (1 - \alpha) \times \mathbf{c}_{1:T}, \\ \alpha = & \text{Softmax}(\mathcal{AT}(\mathbf{r}_{1:T}, \mathbf{c}_{1:T})), \end{aligned} \quad (5)$$

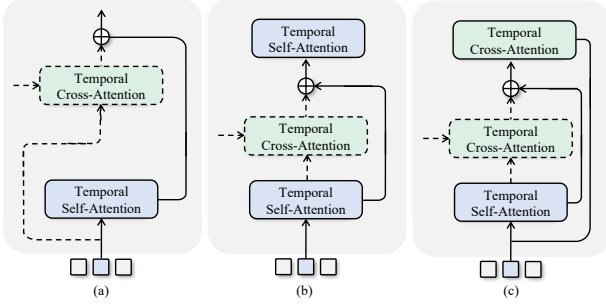


Figure 5. **Comparison of Forward Path Designs.** Straightforward fusion module (a) merges audio features without refined body features and recombines audio features based only on position embedding. The Self-Attention decoder module (b), adopted in previous MLM models [17, 31], is limited for tasks requiring auto-regressive inference. Our design (c) considers effective audio feature fusion and auto-regressive decoding.

where \mathcal{AT} is a 2-layer MLP. We apply two separate CRA encoders for the face and body.

4.3. Masked Audio-Conditioned Gesture Modeling

We propose a Masked Audio Gesture Transformer to leverage different training paths (see Fig. 5 for the motivation behind the architecture designs). Given temporal and spatially masked gestures $\bar{\mathbf{g}} \in \mathbb{R}^{T \times 337}$, we first replace the masked tokens with learned masked embeddings $e_{\text{mask}} \in \mathbb{R}^{256}$, as the value zero still represents specific motion content, e.g., a T-pose. We linearly increase the ratio of masked joints and frames from 0 to 95% according to the training epochs.

A spatial convolutional \mathcal{SC} encoder initially summarizes the spatial information, and compress the spatial feature into $\mathbb{R}^{T \times 256}$. We then employ a temporal self-attention (without feed-forward) \mathcal{TSA} to refine the summarized spatial features

$$\mathbf{h} = \mathcal{TSA}(\mathcal{SC}(\bar{\mathbf{g}}) + \mathbf{p}_t), \quad (6)$$

where $\mathbf{h} \in \mathbb{R}^{T \times 512}$ represents encoded body hints, and \mathbf{p}_t is the sum of a learned speaker embedding and PPE [19]. Then, a straightforward temporal cross-attention Transformer decoder \mathcal{TCAT} is adopted for the reconstructed latent $\hat{\mathbf{q}}_{\text{mg}2\text{g}}$,

$$\hat{\mathbf{q}}_{\text{mg}2\text{g}} = \mathcal{TCAT}(\mathbf{h} + \mathbf{p}_t). \quad (7)$$

We minimize the L1 distance in the latent space,

$$\mathcal{L}_{\text{mg}2\text{g}} = \|\hat{\mathbf{q}}_{\text{mg}2\text{g}} - \mathbf{q}\|. \quad (8)$$

Masked gesture reconstruction encodes effective body hints, with the key being to leverage these body hints for gesture generation. We employ a selective fusion for audio and body hints via a temporal cross-attention \mathcal{TCA} . Subsequently, we use the merged audio-gesture features for audio-conditioned gesture latent reconstruction,

$$\hat{\mathbf{q}}_{\text{a}2\text{g}} = \mathcal{TCAT}(\mathcal{TCA}(\mathbf{h} + \mathbf{p}_t, \mathbf{f}_{\text{body}}), \bar{\mathbf{g}} + \mathbf{p}_t). \quad (9)$$

	Top.-B	Top.-F	Body	Face
VOCA[14]	-	FLAME	-	38.3 ± 5.63
AMASS[46]	SMPL-X	FLAME	42.0 ± 3.60	-
TalkSHOW[65]	SMPL-X	SMPL-X	14.4 ± 2.19	26.1 ± 6.42
BEAT2 (Ours)	SMPL-X	FLAME	43.6 ± 3.38	35.7 ± 5.91

Table 3. **User Preference Win Rate between Existing Datasets.** ‘Top.’ denotes the topology of the mesh. The results show our BEAT2 dataset outperforms the existing PGT dataset [65] in both body and face aspects. It also performs slightly better on body and lower on face when compared with previous mocap [46] and 3D scan-based datasets [14], respectively.

We optimize both the latent code class classification cross-entropy loss $\mathcal{L}_{\text{a}2\text{g-rec}}$ and the latent reconstruction loss $\mathcal{L}_{\text{a}2\text{g-cl}}$ to encourage diverse results.

4.4. Face and Translation Decoding

Considering that the face is weakly related to body motion, applying the same operation – recombining the audio features based on body hints – is not reasonable. Therefore, we directly concatenate the masked body hints with the audio features for the final decoding of facial latent,

$$\hat{\mathbf{q}}_{\text{f}} = \mathcal{TCAT}(\mathbf{f}_{\text{face}} \oplus \mathbf{h}, \mathbf{p}_t). \quad (10)$$

Once we have obtained the local lower body motion $\tilde{\mathbf{g}}_l \in \mathbb{R}^{T \times (54+4)}$ from the VQ-Decoder, we estimate the global translations $\tilde{\mathbf{t}} \in \mathbb{R}^{T \times 3}$ with a pretrained Global Motion Predictor $\hat{\mathbf{t}} = \mathcal{G}(\tilde{\mathbf{g}}_l)$, which significantly reduces foot sliding.

5. Experiments

We separate the evaluation into two categories: dataset quality and model ability. After removing data with low finger quality from BEAT, BEAT2 is reduced to 60 hours. We further split it into BEAT2-Standard (27 hours) and BEAT2-Additional (33 hours), based on the type of speech and conversation sections [39]. While acted gestures in speech sections are more diverse and expressive, spontaneous gestures in conversational sections tend to be more natural yet less varied. We report the results on BEAT2-Standard Speaker-2 with an 85%/7.5%/7.5% train/val/test split.

5.1. Dataset Quality Evaluation

We compare our dataset with the state-of-the-art pseudo ground truth (PGT) dataset, TalkSHOW [65], for both face and body. Additionally, we compare it with the AMASS [46] dataset for the body and VOCA [14] for the face as references. Due to the varying lengths of sequences in each dataset, we sample 100 comparison pairs, each with an equal duration ranging from 2 to 4 seconds. In a perceptual study, each participant evaluates a random set of 40 pairs during a 10-minute session by selecting the sequence they consider to have the best captured quality. In total, 60 participants were invited. It is important to note that participants are instructed to compare only the upper body results,

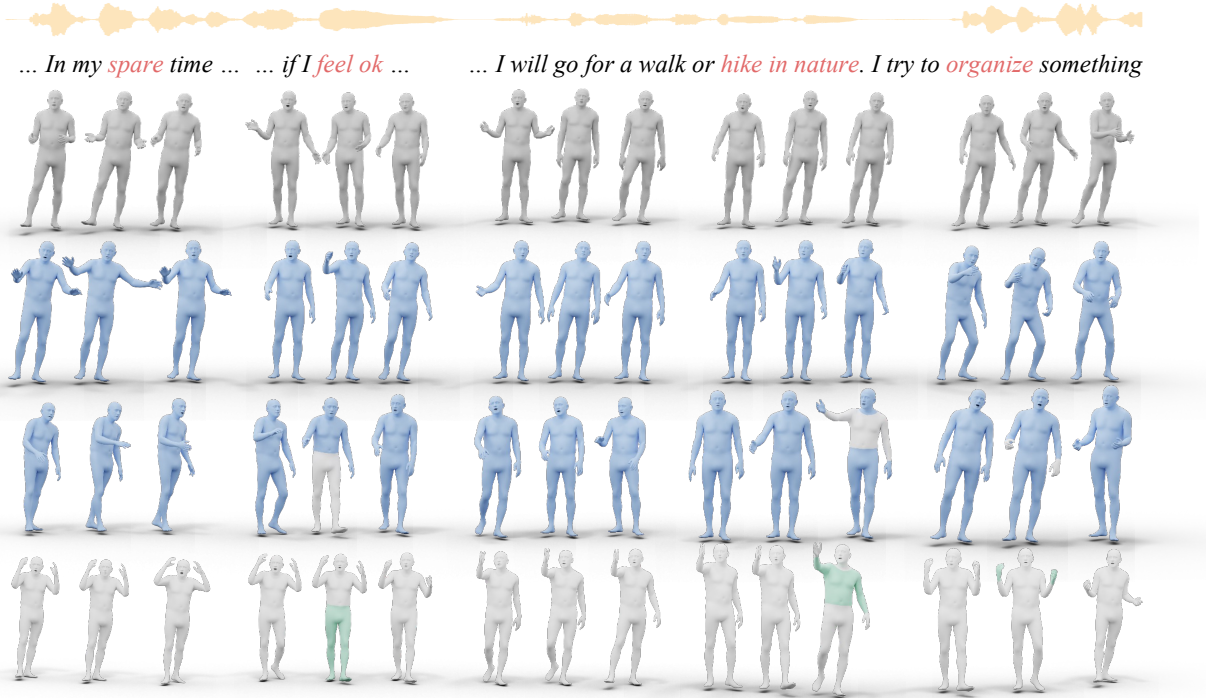


Figure 6. **Subjective Examples.** *Top to down:* GroundTruth, **Generated W/O Body Hints**, **Generated With** Body Hints, **Visible** Body Hints, EMAGE generates diverse, semantic-aware and audio synchronized body gestures, *e.g.* raise the both hands for “spare time”, relaxing gestures for “hike in nature”. Besides, as shown in the third and bottom rows, EMAGE is flexible to accept non-audio-synchronized body hints on any frames and joints, to guide or customize the generated gestures explicitly, *e.g.*, repeat a similar motion for raising hands, change the walking orientations, *etc.* Note that in this figure, The gray joints of generated results are not copies of visible hints.

	FGD ↓	BC ↑	Diversity ↑	MSE ↓	LVD ↓
FaceFormer[19]	-	-	-	7.787	7.593
CodeTalker[61]	-	-	-	8.026	7.766
S2G[25]	28.15	4.683	5.971	-	-
Trimodal[67]	12.41	5.933	7.724	-	-
HA2G[40]	12.32	6.779	8.626	-	-
DisCo[38]	9.417	6.439	9.912	-	-
CaMN[39]	6.644	6.769	10.86	-	-
DiffStyleGesture[62]	8.811	7.241	11.49	-	-
Habibie <i>et al.</i> [28]	9.040	7.716	8.213	8.614	8.043
TalkSHOW[65]	6.209	6.947	13.47	7.791	7.771
EMAGE (Ours)	5.512	7.724	13.06	7.680	7.556

Table 4. **Quantitative evaluation on BEATv2.** We report FGD $\times 10^{-1}$, BC $\times 10^{-1}$, Diversity, MSE $\times 10^{-8}$, and LVD $\times 10^{-5}$. For body gestures, EMAGE significantly improves the FGD, indicating that the generated results are closer to the GT. This shows the effectiveness of body hints from masked gesture modeling.

as TalkSHOW contains only the upper body. The results are shown in Table 3.

5.2. Model Ability Evaluation

We report results using BEATv1.3 and BEATv2. The latter has facial data refined by animators and hand data filtered by annotators.

Metrics. We adopt FGD[67] to evaluate the realism of the body gestures. Then, we measure Diversity[33] by calcu-

	Holistic	Body	Face
Habibie <i>et al.</i> [28]	12.4 \pm 3.70	15.9 \pm 6.49	10.8 \pm 3.19
TalkSHOW[65]	34.9 \pm 5.79	40.4 \pm 8.22	33.2 \pm 6.03
EMAGE (Ours)	52.7 \pm 7.91	44.7 \pm 8.68	56.0 \pm 7.80

Table 5. **User Preference Win Rate On Generated Results.** The results indicate that our generated outcomes are perceived as more realistic and believable, with a 14% and 23% higher user preference for body and face gestures, respectively.

lating the average L1 distance between multiple body gesture clips, and use BC [34] to assess speech-motion synchrony. For the face, we calculate the vertex MSE[61] to measure the positional distance and the vertex L1 difference LVD [65] between the GT and generated facial vertices.

Compared Methods. We first compare our method with representative state-of-the-art methods in body gesture generation [25, 38–40, 62, 67] and talking head generation [19, 61] by reproducing their methods for body and face, respectively. In addition, we reproduce two previous state-of-the-art holistic pipelines, Habibie *et al.* [28] and TalkSHOW [65], whose original implementations are limited to the upper body. We add a lower-body decoder to Habibie *et al.* and a lower-body VQ-VAE to TalkSHOW.

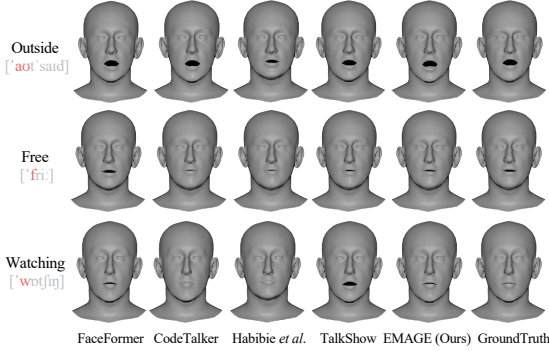


Figure 7. **Comparison of Generated Facial Movements.** Compared with previous state-of-the-art talking face generation methods FaceFormer [19] and CodeTalker [61] as well as holistic gesture generation methods Habibie *et al.* [28] and TalkSHOW [65]. Note that CodeTalker has higher MSE than EMAGE on BEATv2 (Table 4, lower is better) but is subjectively realistic. EMAGE gets good lip motions by leveraging both the face model and masked body hints.

5.2.1 Quantitative and Qualitative Analysis

As shown in Table 4, with a four-frame seed pose, our method outperforms previous SOTA algorithms. For qualitative results, see Figures 6 and 7. Furthermore, we conduct a perceptual study. Maintaining the same setup of 60 participants, each participant evaluates 40 pairs of 10-second results to decide which is most believable; this gives the win rate shown in Table 5.

5.2.2 Ablation Analysis

Performance of Baseline. As shown in Table 6, we start with a teacher-force transformer-based baseline. This baseline, inspired by FaceFormer [19], adopts a 1-layer cross-attention transformer decoder and replaces the audio features from Wav2Vec2 [6] with our custom TCN [7] and trainable word embeddings [9].

Effect of Multiple VQ-VAEs. Simply applying one VQ-VAE [27, 59] for full-body movements, including the face, decreases performance in facial movements. This is because the VQ-VAE is trained to minimize the average loss for the full body, and some speakers’ most frequent movements are not related to the audio. Implementing separated VQ-VAEs allows the model to better leverage the advantages of discrete priors.

Effect of Content Rhythm Self-Attention. Adaptive fusion of rhythm and content features shows improvement in both FGD and Alignment. It selectively focuses the current motion more on rhythm or content features based on the training data’s distribution. Moreover, we observed more semantic-aware results when applying CRA.

Effect of Masked Body Gesture Hints. The improvement across all objective metrics demonstrates that our model effectively leverages spatial-temporal gesture priors, reducing

	FGD ↓	BC ↑	Diversity ↑	MSE ↓	LVD ↓
Ground Truth	0	6.896	13.074	0	0
Reconstruction	3.913	6.758	13.145	0.841	6.389
Baseline	13.080	6.941	8.3145	1.442	9.317
+ VQVAE	9.787	6.673	10.624	1.619	9.473
+ 4 VQVAE	7.397	6.698	12.544	1.243	8.938
+ CRA	6.833	6.783	12.676	1.186	8.715
+ Masked Hints	5.423	6.794	13.057	1.180	9.015

Table 6. **Ablation Analysis on BEATv1.3**

	body	hands	face	FGD ↓	BC ↑	Diversity ↑
BESTX	✓	✓	✓	5.423	6.794	13.057
+ Trinity[22]	✓			5.319	6.843	13.346
+ AMASS[46]	✓	✓		5.174	6.769	14.318

Table 7. **Training EMAGE on Multiple Datasets.** EMAGE demonstrates flexibility by training on multiple datasets, even when only a subset of holistic gestures is available. This approach further improves the objective metrics on the BEATv1.3 test set.

the likelihood of incorrect gesture sampling. Furthermore, masked gesture modeling is key to enabling the network to accept predefined gestures in specific frames.

5.2.3 Ability of Multi-Dataset Training.

We demonstrate that EMAGE can effectively combine multiple non-holistic datasets for training by jointly training with the Trinity [22] and AMASS [46] datasets, by using only the upper body and audio pairs from Trinity and only body and hands from AMASS. Separate VQ-VAEs are trained for BEAT2, Trinity, and AMASS, with separate MLP heads implemented for codebook classification. The results in Table 7 show that incorporating data improves performance on the BEATv1.3 test set.

6. Conclusion

In this work, we present EMAGE, a framework designed to accept partial gestures as input for completing audio-synchronized holistic gestures. It demonstrates that leveraging masked gesture reconstruction can significantly enhance the performance of audio-conditioned gesture generation. Furthermore, the design of EMAGE enables the training on multiple datasets, further improving performance. Alongside EMAGE, we release BEAT2, the largest multi-modal gesture dataset consistent with SMPL-X and FLAME. We hope that BEAT2 will contribute to knowledge and model sharing across various subareas.

Disclosures: While You Zhou, Xuefei Zhe, Naoya Iwamoto, and Bo Zheng are employees of Huawei Tokyo Research Center, this work was done on their own time with the approval of their employer. MJB CoI: https://files.is.tue.mpg.de/black/CoI_CVPR_2024.txt

References

- [1] Kfir Aberman, Peizhuo Li, Dani Lischinski, Olga Sorkine-Hornung, Daniel Cohen-Or, and Baoquan Chen. Skeleton-aware networks for deep motion retargeting. *ACM Transactions on Graphics (TOG)*, 39(4):62–1, 2020. 2
- [2] Chaitanya Ahuja, Dong Won Lee, Yukiko I Nakano, and Louis-Philippe Morency. Style transfer for co-speech gesture animation: A multi-speaker conditional-mixture approach. In *European Conference on Computer Vision*, pages 248–265. Springer, 2020. 2
- [3] Simon Alexanderson, Gustav Eje Henter, Taras Kucherenko, and Jonas Beskow. Style-controllable speech-driven gesture synthesis using normalising flows. In *Computer Graphics Forum*, pages 487–496. Wiley Online Library, 2020. 2
- [4] Tenglong Ao, Zeyi Zhang, and Libin Liu. Gesturediffclip: Gesture diffusion model with clip latents. *ACM Trans. Graph.* 2, 5
- [5] Tenglong Ao, Qingzhe Gao, Yuke Lou, Baoquan Chen, and Libin Liu. Rhythmic gesticulator: Rhythm-aware co-speech gesture synthesis with hierarchical neural embeddings. *ACM Transactions on Graphics (TOG)*, 41(6):1–19, 2022. 2, 3
- [6] Alexei Baevski, Yuhao Zhou, Abdelrahman Mohamed, and Michael Auli. wav2vec 2.0: A framework for self-supervised learning of speech representations. *Advances in neural information processing systems*, 33:12449–12460, 2020. 8
- [7] Shaojie Bai, J Zico Kolter, and Vladlen Koltun. An empirical evaluation of generic convolutional and recurrent networks for sequence modeling. arxiv 2018. *arXiv preprint arXiv:1803.01271*, 2, 1803. 8
- [8] Gilad Baruch, Zhuoyuan Chen, Afshin Dehghan, Tal Dimry, Yuri Feigin, Peter Fu, Thomas Gebauer, Brandon Joffe, Daniel Kurz, Arik Schwartz, and Elad Shulman. ARKitScenes - a diverse real-world dataset for 3d indoor scene understanding using mobile RGB-d data. In *Thirty-fifth Conference on Neural Information Processing Systems Datasets and Benchmarks Track (Round 1)*, 2021. 2, 3
- [9] Piotr Bojanowski, Edouard Grave, Armand Joulin, and Tomas Mikolov. Enriching word vectors with subword information. *Transactions of the association for computational linguistics*, 5:135–146, 2017. 5, 8
- [10] Biovision BVH. Biovision bvh. In <https://research.cs.wisc.edu/graphics/Courses/cs-838-1999/Jeff/BVH.html>, 1999. 3
- [11] Zhe Cao, Gines Hidalgo, Tomas Simon, Shih-En Wei, and Yaser Sheikh. Openpose: realtime multi-person 2d pose estimation using part affinity fields. *IEEE transactions on pattern analysis and machine intelligence*, 43(1):172–186, 2019. 2
- [12] Zhe Chen, Yuchen Duan, Wenhai Wang, Junjun He, Tong Lu, Jifeng Dai, and Yu Qiao. Vision transformer adapter for dense predictions. *arXiv preprint arXiv:2205.08534*, 2022. 3
- [13] Kiran Chhatre, Radek Daněček, Nikos Athanasiou, Giorgio Becherini, Christopher Peters, Michael J Black, and Timo Bolkart. Emotional speech-driven 3d body animation via disentangled latent diffusion. *arXiv preprint arXiv:2312.04466*, 2023. 1
- [14] Daniel Cudeiro, Timo Bolkart, Cassidy Laidlaw, Anurag Ranjan, and Michael Black. Capture, learning, and synthesis of 3D speaking styles. *Computer Vision and Pattern Recognition (CVPR)*, pages 10101–10111, 2019. 2, 3, 6
- [15] Radek Daněček, Kiran Chhatre, Shashank Tripathi, Yandong Wen, Michael Black, and Timo Bolkart. Emotional speech-driven animation with content-emotion disentanglement. ACM, 2023. 1
- [16] Anna Deichler, Kiran Chhatre, Christopher Peters, and Jonas Beskow. Spatio-temporal priors in 3d human motion. 2021. 2
- [17] Jacob Devlin, Ming-Wei Chang, Kenton Lee, and Kristina Toutanova. Bert: Pre-training of deep bidirectional transformers for language understanding. *arXiv preprint arXiv:1810.04805*, 2018. 3, 6
- [18] Alexey Dosovitskiy, Lucas Beyer, Alexander Kolesnikov, Dirk Weissenborn, Xiaohua Zhai, Thomas Unterthiner, Mostafa Dehghani, Matthias Minderer, Georg Heigold, Sylvain Gelly, et al. An image is worth 16x16 words: Transformers for image recognition at scale. *arXiv preprint arXiv:2010.11929*, 2020. 3
- [19] Yingruo Fan, Zhaojiang Lin, Jun Saito, Wenping Wang, and Taku Komura. Faceformer: Speech-driven 3d facial animation with transformers. In *Proceedings of the IEEE/CVF Conference on Computer Vision and Pattern Recognition (CVPR)*, 2022. 2, 3, 6, 7, 8
- [20] Yingruo Fan, Zhaojiang Lin, Jun Saito, Wenping Wang, and Taku Komura. Faceformer: Speech-driven 3d facial animation with transformers. In *Proceedings of the IEEE/CVF Conference on Computer Vision and Pattern Recognition*, pages 18770–18780, 2022. 1
- [21] Gabriele Fanelli, Juergen Gall, Harald Romsdorfer, Thibaut Weise, and Luc Van Gool. A 3-d audio-visual corpus of affective communication. *IEEE Transactions on Multimedia*, 12(6):591–598, 2010. 2
- [22] Ylva Ferstl and Rachel McDonnell. Investigating the use of recurrent motion modelling for speech gesture generation. In *Proceedings of the 18th International Conference on Intelligent Virtual Agents*, pages 93–98, 2018. 3, 8
- [23] Erik Gärtner, Mykhaylo Andriluka, Erwin Coumans, and Cristian Sminchisescu. Differentiable dynamics for articulated 3d human motion reconstruction. In *Proceedings of the IEEE/CVF Conference on Computer Vision and Pattern Recognition*, pages 13190–13200, 2022. 2
- [24] Saeed Ghorbani, Ylva Ferstl, Daniel Holden, Nikolaus F. Troje, and Marc-André Carbonneau. Zeroeggs: Zero-shot example-based gesture generation from speech. *Computer Graphics Forum*, 42(1):206–216, 2023. 2, 3
- [25] Shiry Ginosar, Amir Bar, Gefen Kohavi, Caroline Chan, Andrew Owens, and Jitendra Malik. Learning individual styles of conversational gesture. In *Proceedings of the IEEE/CVF Conference on Computer Vision and Pattern Recognition*, pages 3497–3506, 2019. 1, 2, 3, 7
- [26] Yuan Gong, Yu-An Chung, and James Glass. Ast: Audio spectrogram transformer. *arXiv preprint arXiv:2104.01778*, 2021. 3

- [27] Chuan Guo, Xinxin Zuo, Sen Wang, and Li Cheng. Tm2t: Stochastic and tokenized modeling for the reciprocal generation of 3d human motions and texts. In *European Conference on Computer Vision*, pages 580–597. Springer, 2022. 8, 4
- [28] Ikhsanul Habibie, Weipeng Xu, Dushyant Mehta, Lingjie Liu, Hans-Peter Seidel, Gerard Pons-Moll, Mohamed Elgharib, and Christian Theobalt. Learning speech-driven 3d conversational gestures from video. *arXiv preprint arXiv:2102.06837*, 2021. 1, 2, 3, 7, 8
- [29] Kaiming He, Xinlei Chen, Saining Xie, Yanghao Li, Piotr Dollár, and Ross Girshick. Masked autoencoders are scalable vision learners. In *Proceedings of the IEEE/CVF conference on computer vision and pattern recognition*, pages 16000–16009, 2022. 3
- [30] Catalin Ionescu, Dragos Papava, Vlad Olaru, and Cristian Sminchisescu. Human3. 6m: Large scale datasets and predictive methods for 3d human sensing in natural environments. *IEEE transactions on pattern analysis and machine intelligence*, 36(7):1325–1339, 2013. 2
- [31] Zhenzhong Lan, Mingda Chen, Sebastian Goodman, Kevin Gimpel, Piyush Sharma, and Radu Soricut. Albert: A lite bert for self-supervised learning of language representations. *arXiv preprint arXiv:1909.11942*, 2019. 3, 6
- [32] Gilwoo Lee, Zhiwei Deng, Shugao Ma, Takaaki Shiratori, Siddhartha S Srinivasa, and Yaser Sheikh. Talking with hands 16.2 m: A large-scale dataset of synchronized body-finger motion and audio for conversational motion analysis and synthesis. In *Proceedings of the IEEE/CVF International Conference on Computer Vision*, pages 763–772, 2019. 2, 3
- [33] Jing Li, Di Kang, Wenjie Pei, Xuefei Zhe, Ying Zhang, Zhenyu He, and Linchao Bao. Audio2gestures: Generating diverse gestures from speech audio with conditional variational autoencoders. In *Proceedings of the IEEE/CVF International Conference on Computer Vision*, pages 11293–11302, 2021. 1, 2, 7, 3
- [34] Ruilong Li, Shan Yang, David A Ross, and Angjoo Kanazawa. Ai choreographer: Music conditioned 3d dance generation with aist++. In *Proceedings of the IEEE/CVF International Conference on Computer Vision*, pages 13401–13412, 2021. 7, 2
- [35] Tianye Li, Timo Bolkart, Michael J. Black, Hao Li, and Javier Romero. Learning a model of facial shape and expression from 4D scans. *ACM Transactions on Graphics, (Proc. SIGGRAPH Asia)*, 36(6):194:1–194:17, 2017. 2, 3
- [36] Haiyang Liu and Cheng Zhang. Reinforcement learning based neural architecture search for audio tagging. In *2020 International Joint Conference on Neural Networks (IJCNN)*, pages 1–8. IEEE, 2020. 3
- [37] Haiyang Liu and Jihan Zhang. Improving ultrasound tongue image reconstruction from lip images using self-supervised learning and attention mechanism. *arXiv preprint arXiv:2106.11769*, 2021. 3
- [38] Haiyang Liu, Naoya Iwamoto, Zihao Zhu, Zhengqing Li, You Zhou, Elif Bozkurt, and Bo Zheng. Disco: Disentangled implicit content and rhythm learning for diverse co-speech gestures synthesis. In *Proceedings of the 30th ACM International Conference on Multimedia*, pages 3764–3773, 2022. 2, 3, 7
- [39] Haiyang Liu, Zihao Zhu, Naoya Iwamoto, Yichen Peng, Zhengqing Li, You Zhou, Elif Bozkurt, and Bo Zheng. Beat: A large-scale semantic and emotional multi-modal dataset for conversational gestures synthesis. *arXiv preprint arXiv:2203.05297*, 2022. 1, 2, 3, 4, 6, 7
- [40] Xian Liu, Qianyi Wu, Hang Zhou, Yinghao Xu, Rui Qian, Xinyi Lin, Xiaowei Zhou, Wayne Wu, Bo Dai, and Bolei Zhou. Learning hierarchical cross-modal association for co-speech gesture generation. In *Proceedings of the IEEE/CVF Conference on Computer Vision and Pattern Recognition*, pages 10462–10472, 2022. 2, 3, 7
- [41] Xian Liu, Qianyi Wu, Hang Zhou, Yinghao Xu, Rui Qian, Xinyi Lin, Xiaowei Zhou, Wayne Wu, Bo Dai, and Bolei Zhou. Learning hierarchical cross-modal association for co-speech gesture generation. In *Proceedings of the IEEE/CVF Conference on Computer Vision and Pattern Recognition*, pages 10462–10472, 2022. 1, 2
- [42] Yinhan Liu, Myle Ott, Naman Goyal, Jingfei Du, Mandar Joshi, Danqi Chen, Omer Levy, Mike Lewis, Luke Zettlemoyer, and Veselin Stoyanov. Roberta: A robustly optimized bert pretraining approach. *arXiv preprint arXiv:1907.11692*, 2019. 3
- [43] Ze Liu, Yutong Lin, Yue Cao, Han Hu, Yixuan Wei, Zheng Zhang, Stephen Lin, and Baining Guo. Swin transformer: Hierarchical vision transformer using shifted windows. In *Proceedings of the IEEE/CVF international conference on computer vision*, pages 10012–10022, 2021. 3
- [44] Matthew M. Loper, Naureen Mahmood, and Michael J. Black. MoSh: Motion and shape capture from sparse markers. *ACM Transactions on Graphics, (Proc. SIGGRAPH Asia)*, 33(6):220:1–220:13, 2014. 2
- [45] Shuhong Lu, Youngwoo Yoon, and Andrew Feng. Co-speech gesture synthesis using discrete gesture token learning. *arXiv preprint arXiv:2303.12822*, 2023. 2, 3
- [46] Naureen Mahmood, Nima Ghorbani, Nikolaus F. Troje, Gerard Pons-Moll, and Michael J. Black. AMASS: Archive of motion capture as surface shapes. In *International Conference on Computer Vision*, pages 5442–5451, 2019. 2, 3, 6, 8
- [47] Tim Massey. Vicon study of dynamic object tracking accuracy. In <https://www.vicon.com/resources/blog/vicon-study-of-dynamic-object-tracking-accuracy/>, 2020. 2, 3
- [48] Evonne Ng, Shiry Ginosar, Trevor Darrell, and Hanbyul Joo. Body2hands: Learning to infer 3d hands from conversational gesture body dynamics. *Proceedings of the IEEE/CVF Conference on Computer Vision and Pattern Recognition*, pages 11865–11874, 2021. 2, 3
- [49] Kunkun Pang, Dafei Qin, Yingruo Fan, Julian Habekost, Takaaki Shiratori, Junichi Yamagishi, and Taku Komura. Bodyformer: Semantics-guided 3d body gesture synthesis with transformer. *ACM Transactions on Graphics (TOG)*, 42(4):1–12, 2023. 2, 3
- [50] Georgios Pavlakos, Vasileios Choutas, Nima Ghorbani, Timo Bolkart, Ahmed A. A. Osman, Dimitrios Tzionas, and Michael J. Black. Expressive body capture: 3D hands, face,

- and body from a single image. In *Proceedings IEEE Conf on Computer Vision and Pattern Recognition (CVPR)*, pages 10975–10985, 2019. 2, 3, 4
- [51] Ziqiao Peng, Haoyu Wu, Zhenbo Song, Hao Xu, Xiangyu Zhu, Jun He, Hongyan Liu, and Zhaoxin Fan. Emotalk: Speech-driven emotional disentanglement for 3d face animation. In *Proceedings of the IEEE/CVF International Conference on Computer Vision*, pages 20687–20697, 2023. 2
- [52] Mathis Petrovich, Michael J Black, and Gül Varol. Action-conditioned 3d human motion synthesis with transformer vae. In *Proceedings of the IEEE/CVF International Conference on Computer Vision*, pages 10985–10995, 2021. 2
- [53] Xingqun Qi, Chen Liu, Lincheng Li, Jie Hou, Haoran Xin, and Xin Yu. Emotiongesture: Audio-driven diverse emotional co-speech 3d gesture generation. *arXiv preprint arXiv:2305.18891*, 2023. 2
- [54] Xingqun Qi, Jiahao Pan, Peng Li, Ruibin Yuan, Xiaowei Chi, Mengfei Li, Wenhan Luo, Wei Xue, Shanghang Zhang, Qifeng Liu, et al. Weakly-supervised emotion transition learning for diverse 3d co-speech gesture generation. *arXiv preprint arXiv:2311.17532*, 2023. 2
- [55] Guocheng Qian, Xingdi Zhang, Abdullah Hamdi, and Bernard Ghanem. Pix4point: Image pretrained transformers for 3d point cloud understanding. 2022. 3
- [56] Alexander Richard, Michael Zollhöfer, Yandong Wen, Fernando De la Torre, and Yaser Sheikh. Meshtalk: 3d face animation from speech using cross-modality disentanglement. In *Proceedings of the IEEE/CVF International Conference on Computer Vision*, pages 1173–1182, 2021. 2, 3
- [57] Kaede Shiohara, Xingchao Yang, and Takafumi Taketomi. Blendface: Re-designing identity encoders for face-swapping. In *Proceedings of the IEEE/CVF International Conference on Computer Vision*, pages 7634–7644, 2023. 2
- [58] Tommi Tykkälä, Cédric Audras, and Andrew I Comport. Direct iterative closest point for real-time visual odometry. In *2011 IEEE International Conference on Computer Vision Workshops (ICCV Workshops)*, pages 2050–2056. IEEE, 2011. 5
- [59] Aaron Van Den Oord, Oriol Vinyals, et al. Neural discrete representation learning. *Advances in neural information processing systems*, 30, 2017. 5, 8
- [60] Kaisiyuan Wang, Qianyi Wu, Linsen Song, Zhuoqian Yang, Wayne Wu, Chen Qian, Ran He, Yu Qiao, and Chen Change Loy. Mead: A large-scale audio-visual dataset for emotional talking-face generation. In *ECCV*, 2020. 2
- [61] Jinbo Xing, Menghan Xia, Yuechen Zhang, Xiaodong Cun, Jue Wang, and Tien-Tsin Wong. Codetalker: Speech-driven 3d facial animation with discrete motion prior. In *Proceedings of the IEEE/CVF Conference on Computer Vision and Pattern Recognition*, pages 12780–12790, 2023. 1, 2, 3, 4, 7, 8
- [62] Sicheng Yang, Zhiyong Wu, Minglei Li, Zhensong Zhang, Lei Hao, Weihong Bao, Ming Cheng, and Long Xiao. Diffusestylegesture: Stylized audio-driven co-speech gesture generation with diffusion models. *arXiv preprint arXiv:2305.04919*, 2023. 2, 3, 7
- [63] Xingchao Yang and Takafumi Taketomi. Bareskinnet: De-makeup and de-lighting via 3d face reconstruction. In *Computer Graphics Forum*, pages 623–634. Wiley Online Library, 2022. 2
- [64] Xingchao Yang, Takafumi Taketomi, and Yoshihiro Kanamori. Makeup extraction of 3d representation via illumination-aware image decomposition. In *Computer Graphics Forum*, pages 293–307. Wiley Online Library, 2023. 2
- [65] Hongwei Yi, Hualin Liang, Yifei Liu, Qiong Cao, Yandong Wen, Timo Bolkart, Dacheng Tao, and Michael J Black. Generating holistic 3d human motion from speech. In *CVPR*, 2023. 1, 2, 3, 4, 5, 6, 7, 8
- [66] Youngwoo Yoon, Woo-Ri Ko, Minsu Jang, Jaeyeon Lee, Jaehong Kim, and Geehyuk Lee. Robots learn social skills: End-to-end learning of co-speech gesture generation for humanoid robots. In *2019 International Conference on Robotics and Automation (ICRA)*, pages 4303–4309. IEEE, 2019. 2, 3
- [67] Youngwoo Yoon, Bok Cha, Joo-Haeng Lee, Minsu Jang, Jaeyeon Lee, Jaehong Kim, and Geehyuk Lee. Speech gesture generation from the trimodal context of text, audio, and speaker identity. *ACM Transactions on Graphics (TOG)*, 39(6):1–16, 2020. 1, 2, 3, 7
- [68] Xumin Yu, Lulu Tang, Yongming Rao, Tiejun Huang, Jie Zhou, and Jiwen Lu. Point-bert: Pre-training 3d point cloud transformers with masked point modeling. In *Proceedings of the IEEE/CVF Conference on Computer Vision and Pattern Recognition*, pages 19313–19322, 2022. 3
- [69] Hengshuang Zhao, Li Jiang, Jiaya Jia, Philip HS Torr, and Vladlen Koltun. Point transformer. In *Proceedings of the IEEE/CVF international conference on computer vision*, pages 16259–16268, 2021. 3
- [70] Yihao Zhi, Xiaodong Cun, Xuelin Chen, Xi Shen, Wen Guo, Shaoli Huang, and Shenghua Gao. Livelyspeaker: Towards semantic-aware co-speech gesture generation. In *Proceedings of the IEEE/CVF International Conference on Computer Vision (ICCV)*, pages 20807–20817, 2023. 2, 3
- [71] Yang Zhou, Jimei Yang, Dingzeyu Li, Jun Saito, Deepali Aneja, and Evangelos Kalogerakis. Audio-driven neural gesture reenactment with video motion graphs. In *Proceedings of the IEEE/CVF Conference on Computer Vision and Pattern Recognition*, pages 3418–3428, 2022. 2
- [72] Lingting Zhu, Xian Liu, Xuanyu Liu, Rui Qian, Ziwei Liu, and Lequan Yu. Taming diffusion models for audio-driven co-speech gesture generation. In *Proceedings of the IEEE/CVF Conference on Computer Vision and Pattern Recognition*, pages 10544–10553, 2023. 2, 3
- [73] Wentao Zhu, Xiaoxuan Ma, Zhaoyang Liu, Libin Liu, Wayne Wu, and Yizhou Wang. Motionbert: A unified perspective on learning human motion representations. In *Proceedings of the IEEE/CVF International Conference on Computer Vision*, 2023. 3

EMAGE: Towards Unified Holistic Co-Speech Gesture Generation via Expressive Masked Audio Gesture Modeling

Supplementary Material

This supplemental document contains seven sections:

- Evaluation Metrics (Section A).
- BEAT2 Dataset Details (Section B).
- Baselines Reproduction Details (Section C).
- Settings of EMAGE (Section D).
- Visualization Blender Addon (Section E).
- Training time (Section F).
- Importance of lower body motion (Section G).

A. Evaluation Metrics

Fréchet Gesture Distance. A lower FGD, as referenced by [67], indicates that the distribution between the ground truth and generated body gestures is closer. Similar to the perceptual loss used in image generation tasks, FGD is calculated based on latent features extracted by a pretrained network,

$$\text{FGD}(\mathbf{g}, \hat{\mathbf{g}}) = \|\mu_r - \mu_g\|^2 + \text{Tr}(\Sigma_r + \Sigma_g - 2(\Sigma_r \Sigma_g)^{1/2}), \quad (11)$$

where μ_r and Σ_r represent the first and second moments of the latent features distribution z_r of real human gestures \mathbf{g} , and μ_g and Σ_g represent the first and second moment of the latent features distribution z_g of generated gestures $\hat{\mathbf{g}}$. We use a Skeleton CNN (SKCNN) based encoder [1] and a Full CNN-based decoder as the autoencoder pretrained network. The network is pretrained on both BEAT2-Standard and BEAT2-Additional Data. The choice of SKCNN over a Full CNN encoder is due to its enhanced capability in capturing gesture features, as indicated by a lower reconstruction MSE loss (0.095 compared to 0.103).

L1 Diversity. A higher Diversity [33] indicates a larger variance in the given gesture clips. We calculate the average L1 distance from different N motion clips as follows:

$$\text{L1 div.} = \frac{1}{2N(N-1)} \sum_{t=1}^N \sum_{j=1}^N \left\| p_t^i - \hat{p}_t^j \right\|_1, \quad (12)$$

where p_t represents the position of joints in frame t . We calculate diversity on the entire test dataset. Additionally, to compute joint positions, the translation is set to zero, implying that L1 Diversity is focused solely on local motion.

Beat Constancy (BC). A higher BC, as defined by [34], suggests a closer alignment between the gesture’s rhythm and the beat of the audio. We identify the beginning of speech as the audio beat and consider the local minima of the velocity of the upper body joints (excluding fingers) as the motion beat. The synchronization between audio and gesture is computed in the following manner:

$$\text{BC} = \frac{1}{g} \sum_{b_g \in g} \exp\left(-\frac{\min_{b_a \in a} \|b_g - b_a\|^2}{2\sigma^2}\right), \quad (13)$$

where g and a represent the sets of gesture beat and audio beat, respectively.

B. BEAT2 Dataset Details

Statistics. The original BEAT dataset, as described by [39], contains 76 hours of data for 30 speakers. We exclude speakers 8, 14, 19, 23, and 29, which account for 16 hours of data, due to noise in the finger data, leaving 60 hours of data for 25 speakers (12 female and 13 male). The speech and conversation portions are categorized into BEAT2-standard and BEAT2-additional, containing 27 and 33 hours respectively. We adopt an 85%, 7.5%, and 7.5% split for BEAT2-standard, maintaining the same ratio for each speaker. BEAT2-additional is utilized for further improving the network’s robustness. The results presented in this paper are based on training with BEAT2-standard speaker-2 only. The dataset includes 1762 sequences with an average length of 65.66 seconds per sequence. Each recording in a sequence is a continuous answer to a daily question. Additionally, we report a comparison between TalkShow [65] and our dataset in terms of Diversity and Beat Constancy (BC), as shown in Table 8.

Table 8. **Diversity and BC Comparisons.** The local and global diversity refers to the variance in joint positions with and without global translations, respectively.

	BC \uparrow	Diversity-L \uparrow	Diversity-G \uparrow
TalkShow [65]	6.104	5.273	5.273
BEAT2 (Ours)	6.896	13.074	27.541

Loss Terms of MoSh++. MoSh’s optimization involves loss functions including a Data Term, Surface Distance Energy, Marker Initialization Regularization, Pose and Shape Priors, and a Velocity Constancy Term, which are described as follows:

- Data Term (E_D): Minimizing the squared distance between simulated and observed markers. In the given context, the \tilde{M} , β , Θ , and Γ represent the latent markers, body shape, poses, and body location respectively:

$$E_D(\tilde{M}, \beta, \Theta, \Gamma) = \sum_{i,t} \|\hat{m}(\tilde{m}_i, \beta, \theta_t, \gamma_t) - m_{i,t}\|^2. \quad (14)$$

- Surface Distance Energy (E_S): Ensuring markers main-

tain prescribed distances from the body surface:

$$E_S(\beta, \tilde{M}) = \sum_i \|r(\tilde{m}_i, S(\beta, \theta_0, \gamma_0)) - d_i\|^2. \quad (15)$$

- **Marker Initialization Regularization (E_I):** Penalizing deviations of estimated markers from initial positions:

$$E_I(\beta, \tilde{M}) = \sum_i \|\tilde{m}_i - v_i(\beta)\|^2. \quad (16)$$

- **Pose and Shape Priors:** Penalizing deviations from mean shape and pose:

$$E_\beta(\beta) = (\beta - \mu_\beta)^T \Sigma_\beta^{-1} (\beta - \mu_\beta), \quad (17)$$

$$E_\theta(\Theta) = \sum_t (\theta_t - \mu_\theta)^T \Sigma_\theta^{-1} (\theta_t - \mu_\theta). \quad (18)$$

- **Velocity Constancy Term (E_u):** Reducing marker noise and ensuring movement consistency:

$$E_u(\Theta) = \sum_{t=2}^n \|\theta_t - 2\theta_{t-1} + \theta_{t-2}\|^2. \quad (19)$$

The overall objective function is the weighted sum of these terms, balancing accuracy and plausibility:

$$E(\tilde{M}, \beta, \Theta, \Gamma) = \sum_{\omega \in \{D, S, \theta, \beta, I, u\}} \lambda_\omega E_\omega(\cdot). \quad (20)$$

More details and pseudo code of the head and neck shape optimization are available in the code release.

Details of FLAME Parameter Optimization. To animate a face using the SMPL-X model with ARKit parameters from the BEAT dataset, we estimate FLAME expression parameters by minimizing the geometric error between an animated ARKit and FLAME model. Addressing the optimization challenges posed by differing mesh structures, we construct an ARKit-compatible FLAME model utilizing Faceit, a Blender add-on tailored for crafting ARKit blendshapes. By driving the ARKit-aligned FLAME model with each set of ARKit parameters from the BEAT dataset, we obtain original FLAME expression parameters by minimizing the L2 distance loss between equivalent vertices. Finally, the optimized FLAME expression parameters can be directly applied to SMPL-X. For facial identity parameters, we preserve the same identity parameters on SMPL-X after body fitting with MoSh++ [46].

C. Baselines Reproduction Details

Number of Joints. All baseline methods output full-body joint rotations represented by $\mathbf{g} \in \mathbb{R}^{T \times (55 \times 6)}$ and, in addition to rotations, they decode global translations $\in \mathbb{R}^{T \times 3}$.

To provide a thorough comparison, we present subjective results for both the upper body (excluding global motion) and the full body.

Autoregressive Training. We observe that autoregressive training/inference-based models, such as FaceFormer and CodeTalker [19, 61], perform worse than non-autoregressive methods. In non-autoregressive settings, only positional embedding is used as input for cross-attention to audio features, particularly when training with Rot6D and axis-angle representations. The network architecture of FaceFormer and CodeTalker is based on transformers and was initially proposed for training with the representation of vertex offsets. As shown in Table 9, we find that non-autoregressive training improves performance with FLAME’s parameters. The results in this paper are obtained using a non-autoregressive training approach. Non-autoregressive training techniques have also been employed in the training of EMAGE.

Table 9. **Vertex Errors (MSE) with Different Training Methods.** ‘FF’ and ‘CT’ refer to FaceFormer [19] and CodeTalker [61], respectively. ‘TF’, ‘AR’, and ‘NonAR’ represent Teacher-Force, AutoRegressive, and Non-AutoRegressive training, respectively. We train on the VOCA dataset with a vertex loss, and BEAT2 with a FLAME parameter loss combined with a vertex loss. Results indicate that the same method performs differently when using the two representations; in BEAT2, non-autoregressive training demonstrates superior performance. The average MSE is calculated on 5023 and 10475 vertices for VOCA and BEAT2, respectively:

	FF-TF	FF-AR	FF-NonAR	CT-TF	CT-AR	CT-NonAR
VOCA (x10-7)	6.636	6.023	6.138	7.914	7.637	7.541
BEAT2 (x10-7)	2.167	3.704	1.195	2.079	4.120	1.243

Adversarial Training. We omit the adversarial training in Speech2Gesture [25], CaMN [39], and Habibie *et al* [28], because their outputs with adversarial training show noticeable jitter, even when we increase the weight for the velocity loss. Similar effects are also observed in training with 3D data for Speech2Gesture [25], as reported in the study by [33].

Lower Body VQ-VAE for TalkShow. We introduce an additional VQ-VAE for TalkShow, utilizing their autoregressive (AR) model to jointly predict the class index of the upper body, hands, and lower body. The global translations are encoded in conjunction with lower body joints.

D. Settings of EMAGE

Training. We train our method for 400 epochs, gradually increasing the ratio of masked joints from 0 to 95% linearly according to the training epoch. This approach proves more

effective than a fixed masked ratio, such as 25%, based on our experiments. The learning rate is $2.5e-4$, and we use the Adam optimizer with a gradient norm clipped at 0.99 to ensure stable training.

Structure of VQ-VAE. We employ the same CNN-based VQ-VAE [27] for all four body segments. The downsample rate is set to 1 to achieve the best reconstruction quality. We utilize a feature length of 512 for the codebook entries and set the codebook size to 256. The total decoding space for body gestures is represented as $\in \mathbb{R}^{T \times 256^3}$. The VQ-VAE is trained for 200 epochs, with a learning rate of $2.5e-4$ for the initial 195 epochs, which is then decreased to $2.5e-4$ for the last 5 epochs.

Global Motion Predictor. We train the Global Motion Predictor using an architecture that mirrors the CNN-based structure of our VQ-VAE’s encoder and decoder. The input consists of local motions and predicted foot contact labels $\in \mathbb{R}^{T \times 334}$, and it outputs global translations $\in \mathbb{R}^{T \times 3}$.

E. Visualization Blender Add-on

For straightforward visualization of our BEAT2 dataset, we utilize the SMPL-X Blender add-on [50]. As the latest SMPL-X add-on does not support the full range of facial expressions for SMPL-X, we extract 300 expression meshes from the original SMPL-X model and added them as individual blendshape targets into the SMPL-X model within the Blender add-on.

F. Training time

We report the training time on a single L4, V100 and 4090 with a batch size (BS) of 64 for the best performance.

EMAGE	1-speaker		25-speaker		Mem.	BS
	1-epoch	400-epoch	1-epoch	100-epoch		
L4 (24G)	239s	26.5h	3197s	89.6h	20.1G	64
V100 (32G)	155s	17.2h	2073s	58.1h	20.1G	64
4090 (24G)	72s	8.0h	963s	27.1h	20.1G	64

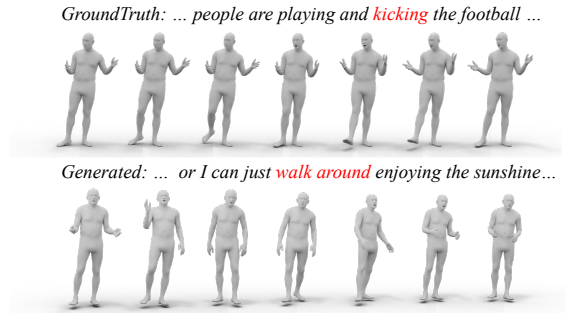
Additionally, pretraining of the $5 \times$ VQVAEs for face, hands, upper body, lower body, and global motion would take 22.4 hours on 5×4090 GPUs.

VQVAEs \times 1	1-speaker		25-speaker		Mem.	BS
	1-epoch	700-epoch	1-epoch	100-epoch		
L4 (24G)	200s	39.5h	2760s	74.4h	13.8G	64
V100 (32G)	131s	25.5h	1727s	48.0h	13.8G	64
4090 (24G)	61s	11.9h	802s	22.4h	13.8G	64

G. Importance of lower body motion

Lower body motion allows gestures **semantically aligned** with the content of the audio to achieve more vivid and impressive results, *e.g.*, “hiking in nature” with a walking gesture, “playing football” with a kicking motion; see figure

below. Compared with the upper body, it is more weakly related to the audio, but it still has connections in the above cases.



In the implementation of EMAGE, we first obtain the latents of different body components with separate MLPs. Then, the lower body motion decoder **leverages all latents of “audio”, “upper body”, and “hands”** for cross-attention based lower-body motion decoding. We have also observed that decoding directly from audio increases diversity but reduces the coherence of the results on BEATv1.3.

	FGD ↓	BC ↑	Diversity ↑	MSE ↓	LVD ↓
audio only	6.209	6.683	13.714	1.183	8.788
audio + upper + hands	5.423	6.794	13.075	1.180	8.715